Distribution of Furamidine Analogues in Tumor Cells: Influence of the Number of Positive Charges

Amélie Lansiaux,[†] Laurent Dassonneville,[†] Michaël Facompré,[†] Arvind Kumar,[‡] Chad E. Stephens,[‡] Miroslav Bajic,[‡] Farial Tanious,[‡] W. David Wilson,[‡] David W. Boykin,[‡] and Christian Bailly*,[†]

INSERM U-524 et Laboratoire de Pharmacologie Antitumorale du Centre Oscar Lambret, IRCL, Place de Verdun, 59045 Lille, France, and Department of Chemistry and Laboratory for Chemical and Biological Sciences, Georgia State University, Atlanta, Georgia 30303

Fluorescence microscopy has been used to study the cellular distribution properties of a series of DNA binding cationic compounds related to the potent antiparasitic drug furamidine (DB75). The compounds tested bear a diphenylfuran or a phenylfuranbenzimidazole unfused aromatic core substituted with one or two amidine or imidazoline groups. The synthesis of five new compounds is reported. The B16 melanoma cell line was used to compare the capacities of mono-, bis-, and tetracations to enter the cell and nuclei. The high-resolution fluorescence pictures show that in the furamidine series, the compounds with two or four positive charges selectively accumulate in the cell nuclei whereas, in most cases, those bearing only one positive charge show reduced cell uptake capacities. One of the monocationic compounds, DB607, distributes in the cytoplasm, possibly in mitochondria, with no distinct nuclear accumulation. In sharp contrast, furamidine and benzimidazole analogues, including the drug DB293 that forms DNA minor groove dimers, efficiently accumulate in the cell nuclei and the intranuclear distribution of these DNA minor groove binders is significantly different from that seen with the DNA intercalating drug propidium iodide. The results suggest that the presence of two amidine terminal groups plays a role in facilitating nuclear accumulation into cells, probably as a result of nucleic acid binding. The determination of DNA melting temperature increases on addition of these compounds supports the importance of DNA binding in nuclear uptake.

Introduction

Furamidine (DB75; Chart 1) is a bis-amidine diphenylfuran derivative endowed with high antimicrobial activities. The drug is most active against *Pneumocystis carinii*, a widely spread pathogen responsible for pneumonia that often infects immunodeficient patients, including those with acquired immune deficiency syndrome. In addition, furamidine is active against diverse, highly infectious parasites such as *Giardia lamblia*, *Plasmodium falciparum*, and *Trypanosoma rhodesience*.[1,2] Recently an amidoxime prodrug of furamidine was selected for clinical evaluation[3] and is currently undergoing phase II clinical trials against human African trypanosomes.

In addition to their antimicrobial properties, certain diphenylfuran derivatives exhibit significant cytotoxic activities. Although furamidine is weakly toxic to human cells, in contrast its imidazoline analogue, furimidazoline (DB60), has shown significant antiproliferative activities against various tumor cell lines, including cells resistant to cisplatinum.[4]

The main cellular target of furamidine and related diphenylfuran analogues is considered to be DNA. On the basis of a number of results, it is assumed that these drugs operate at the nucleic acids level by interfering with DNA-interacting enzymes such as topoisomerases.[5−7] To bind to DNA, the drug must first enter the cell and then reach the nuclear compartment. The mechanism by which such positively charged, highly water-soluble drugs manage to penetrate into cells is unknown at present, as is the influence of compound structure on cell uptake. In this report, we have addressed the issue of cell and nuclear uptake by means of fluorescence microscopy. The strong fluorescence properties of the diphenylfuran provide unique opportunities to investigate their subcellular localization. We chose a series of furamidine analogues that differ by (i) the number of positive charges, from one to four charges, (ii) the structure of the terminal group, either an amidine, a more planar imidazoline group, or an amide alkylamine, and (iii) the nature of the central unfused aromatic system, with a symmetrical diphenylfuran or an asymmetrical phenylfuranbenzimidazole system.

Results

DB75. The high intrinsic fluorescence properties of furamidine (and structurally related compounds) greatly facilitate the fluorescence microscopy assessment of its cellular uptake and intracellular distribution. Figure 1 shows fluorescence images of B16 melanoma cells exposed to DB75. The cells (selected for their extended morphology) were treated with 2 μM DB75 for 18 h at 37 °C, washed, fixed with 2% paraformaldehyde, and then labeled with the green fluorescent dye 3,3-dihexyloxacarbocyanine iodide (20 nM $DiOC_6$) and/or with the red fluorescent dye propidium iodide (0.2 μg/mL PI).

---

* To whom correspondence should be addressed. E-mail: bailly@lille.inserm.fr.
† INSERM U-524.
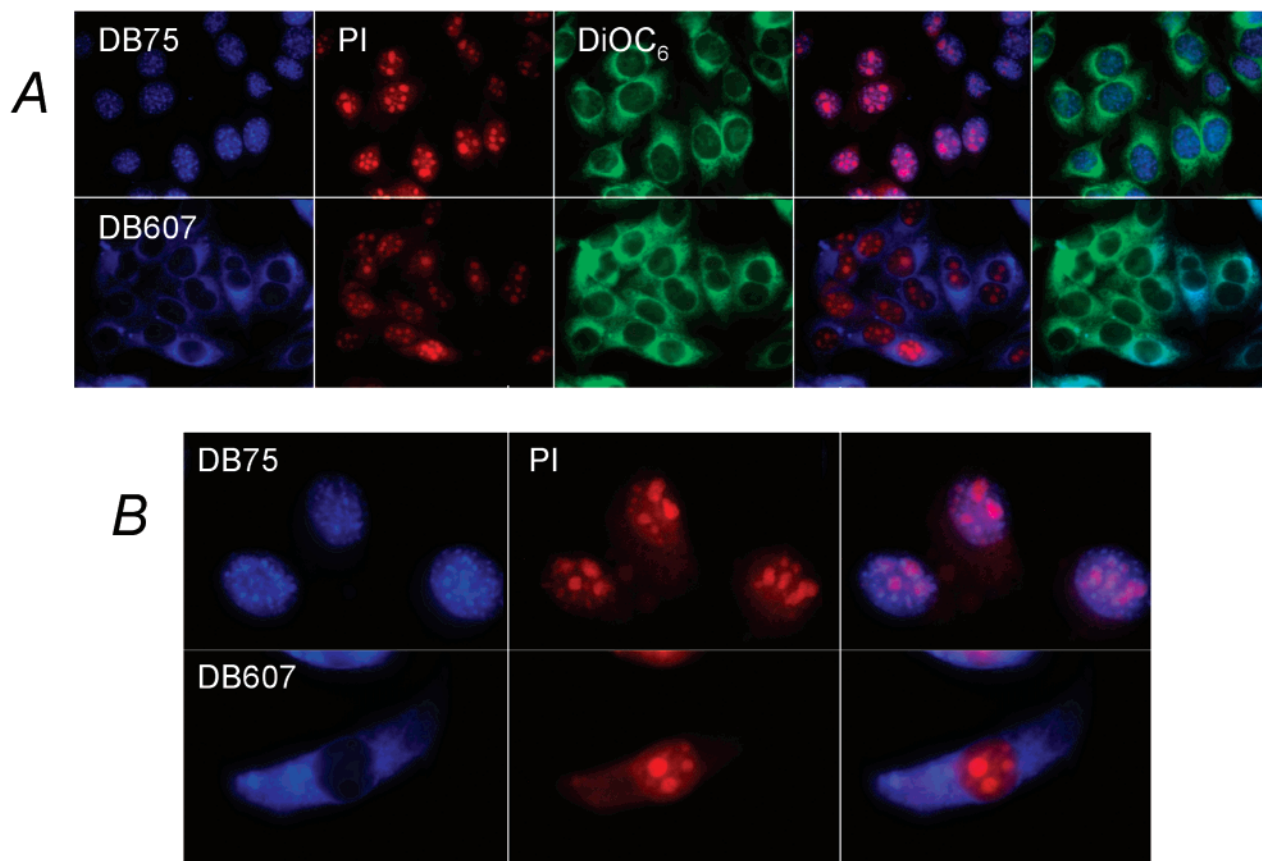‡ Georgia State University.

Figure 1. (A) Fluorescence micrographs of B16 melanoma cells stained with 2 μM DB75 or DB607 (blue) with propidium iodide (PI in red) or with 3,3-dihexyloxacarbocyanine iodide (DiOC$_6$ in green). Images on the right side of the figure show the overlay of the DB compound with PI (blue + red) or with DiOC$_6$ (blue + green). The cells were incubated with the test drug for 18 h, washed, fixed with 2% paraformaldehyde, and then labeled with PI (0.2 μg/mL PI) or DiOC$_6$ (20 nM) prior to the microscopy observation ($\times$63). Panel B shows the cells at a higher magnification ($\times$100) after treatment with 2 μM DB75 or DB607, which accumulate selectively in the nucleus and in the cytoplasm of the cells, respectively. The cells were also stained with PI, and an overlay of the blue and red signals are shown on the right side.

Like ethidium bromide, PI binds strongly to nucleic acids and is routinely used to stain cell nuclei and to label DNA in cytometry studies. In contrast, the DiOC$_6$ dye is known to bind selectively to mitochondria (possibly to reticulum also) and is commonly used to measure variations of the mitochondrial membrane potential,[8] in particular during drug-induced apoptosis.[9,10] Here, DiOC$_6$ was used as a probe to label the cytoplasm of B16 cells. The three colors (blue, green, and red) can be easily differentiated by fluorescence microscopy.

The illustrations in Figure 1A show clearly that essentially all of the DB75 molecules are sequestered in the cell nuclei. The massive accumulation of the blue fluorescence in the nuclear compartment contrasts with the extensive green fluorescence detected in the cytoplasm. Although DB75 essentially colocalizes in the nucleus with PI, the two drugs do not distribute identically within the nucleus of the cells. Significantly distinct intranuclear patterns can be detected (compare the red-blue overlay images in Figure 1A). The differences are very pronounced when the cells are observed at a higher magnification (Figure 1B). A few relatively large and bright-red nucleolar-like bodies were observed with PI, whereas the blue staining with DB75 is more uniformly distributed throughout the nucleus. However, close examination of the micrographs show small puncta that were patchy throughout the nuclei. This different distribution may be due to different DNA sequence selectivity. DB75, but not PI, exhibits a high preference for AT-rich sequences in DNA,[11−13] and therefore, its binding to the GC-rich nature of nucleolar DNA must be disfavored. Altogether, the images in Figure 1 leave no room for doubt that the dicationic compound DB75 accumulates selectively in the cell nuclei and that this process is likely driven by the drug binding to nucleic acids.

Structure Distribution Relationships. Eleven DB75 analogues (Chart 1) were selected to compare their cell distribution profiles. The selected compounds bear a diphenylfuran or a phenylfuranbenzimidazole unfused aromatic core substituted with one or two amidine or imidazoline groups or with two amide alkylamines. They all fluoresce in blue ($\lambda^{exc}_{max} = 360-380$ nm; $\lambda^{em}_{max} = 450-500$ nm), but the relative fluorescence intensity varies with the compound structure. The monocations are less fluorescent than the dications, and therefore, the exposition time (ET in Table 1) had to be adjusted to obtain images of equal intensity. These compounds were specifically chosen to provide some insight into what molecular factors of DB75 play the most significant roles in preventing or favoring cytoplasmic and/or nuclear distribution of the drug.

Figure 2A shows images of (left) three diphenylfuran compounds with one (DB607), two (DB75), and four

Chart 1
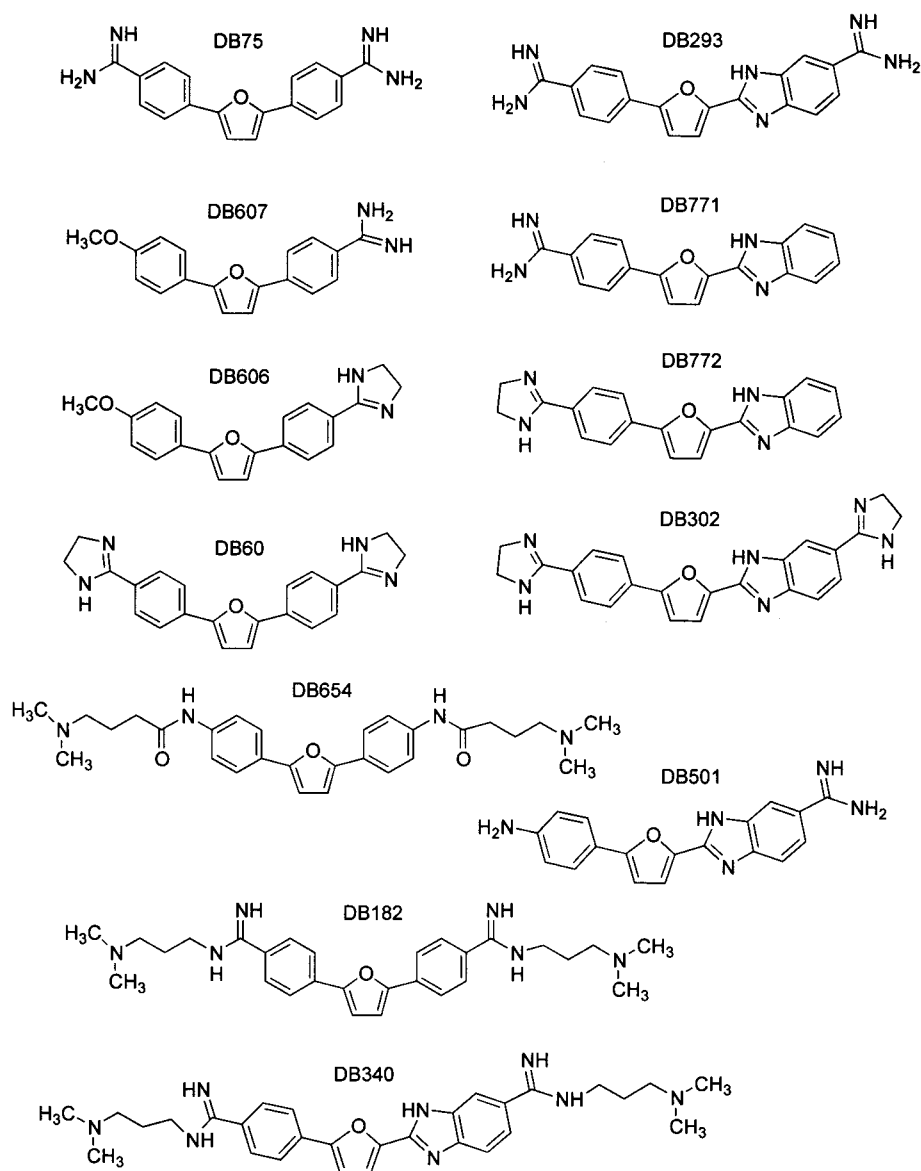
Table 1. Cytotoxicity and DNA Binding

	ET^a (s)	ΔT_m^{b} (°C)	IC$_{50}$^{c} (μM)
DB60	2.3	23.9	1.1 ± 0.06
DB75	0.5	24.7	9.2 ± 0.34
DB182	0.4	>28	2.5 ± 0.85
DB293	0.2	24.0	43.2 ± 1.8
DB302	0.2	>28	nd
DB340	0.4	>28	>100
DB501	13.9	8.9	>100
DB606	20.0	5.2	1.7 ± 0.31
DB607	0.6	5.2	3.5 ± 0.15
DB654	10.0	5.7	2.3 ± 0.40
DB771	6.2	6.9	51.4 ± 2.74
DB772	0.3	8.3	8.6 ± 0.05

^{a} Exposure time required to obtain digital images of equal fluorescence intensity. ^{b} Variation in melting temperature, ΔT_m = $T_m^{complex}$ − T_m^{poly}(dA)·(dT). T_m measurements were performed in MES10 buffer. ^{c} Drug concentration that inhibits B16 cell growth by 50% after 72 h of incubation.

(DB182) positive charges and (right) three phenylfuran-benzimidazole compounds with one (DB771), two (DB293), and four (DB340) positive charges. The pK_a values of benzamidine is sufficiently high (pK_a = 11.2 in 50% EtOH)[14,15] to consider that the studied compounds bear the expected number of positive charges in cells. The dications DB75 and DB293 show identical distribution patterns with their bright-blue fluorescence specifically located in the cell nuclei. The phenyl-to-benzimidazole substitution (DB75 → DB293) profoundly affect DNA sequence recognition[16] but has no detectable effect on cell distribution.

The compounds with only one amidine group show reduced uptake capacities. The monocationic diphenyl-furan derivative DB607 was found essentially in the cytoplasm of the cells. The overlay of the DiOC$_6$ signal and DB607 signal results in a light-blue color where the green and blue signals colocalize. Little or no blue fluorescence was observed in the nuclei. Another set of images obtained with this compound is presented in Figure 1A where the green and red colors are used to show the position of the cytoplasm (DiOC$_6$) and the nucleus (PI), respectively. The uptake differences between DB75 and DB607, which differ only by the nature of one of the terminal groups (amidine vs methoxy), are exemplary. DB75 is clearly inside, whereas DB607 is exclusively outside the nucleus and they produce com-
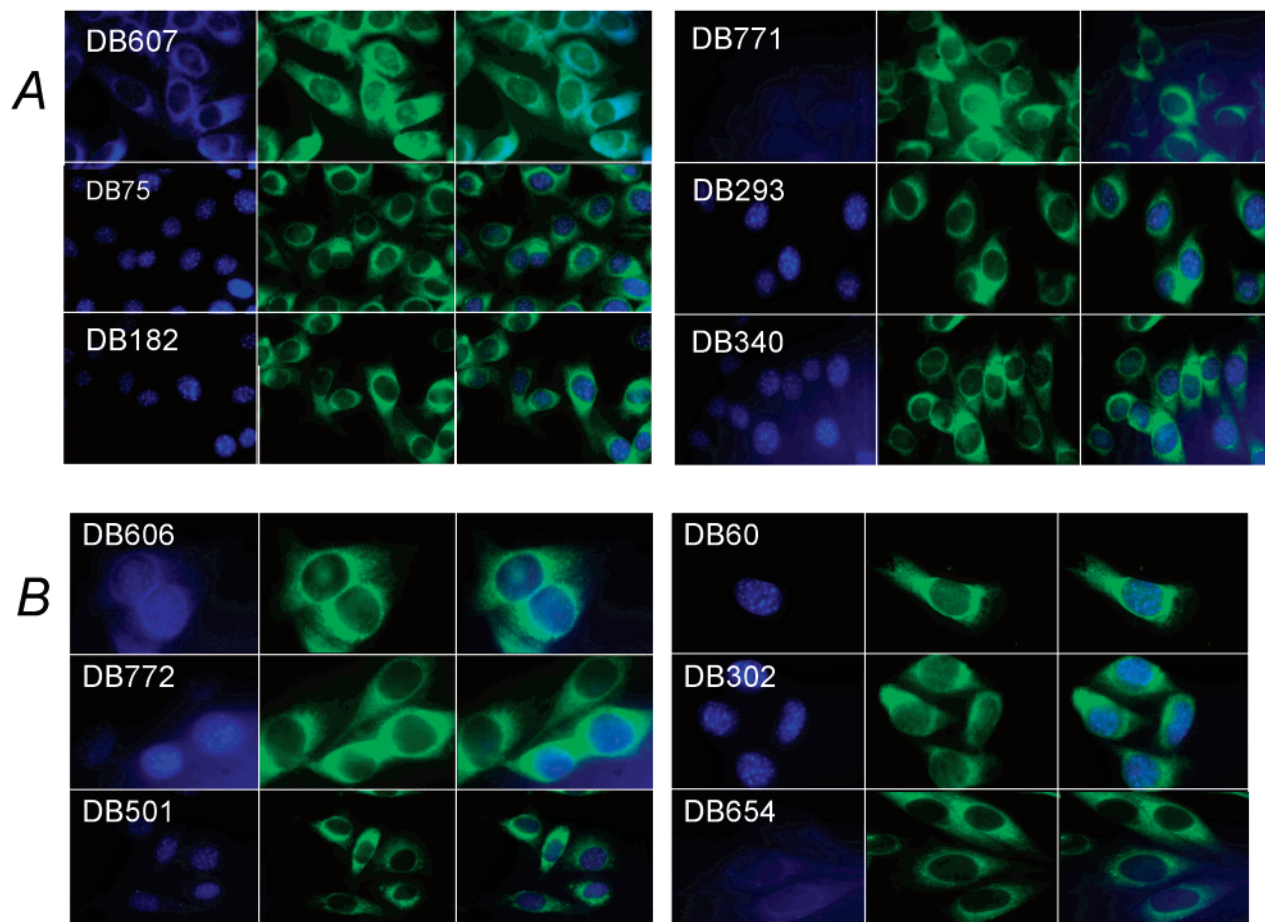
Figure 2. (A) Intracellular distribution of the mono- (DB607, DB771), bis- (DB75, DB293), and tetracationic (DB182, DB340) diphenylfuran (left) and phenylfuranbenzimidazole (right) derivatives (2 μM each) in B16 melanoma cells visualized by fluorescence microscopy ($\times$63) after 18 h of incubation. (B) Intracellular distribution of the monocations (DB606, DB772, DB501) and dications (DB60, DB302, DB654) (2 μM each) in B16 melanoma cells visualized by fluorescence microscopy ($\times$63) after 18 h of incubation. The green images correspond to the subsequent incubation of the same cells with 20 nM $DiOC_6$, and the images on the right side correspond to the superimposed blue + green fluorescence.

pletely opposite distribution patterns in Figure 1A. Figure 1B shows additional views of the cells (at a higher magnification) labeled with the two compounds, allowing full visualization of their totally opposite intracellular spatial distribution. These observations demonstrate that the substitution of a methoxy group in DB607 for one of the amidine groups in DB75 has a major impact on the cell distribution properties of the compound. Conversion of the amidine to a $-OCH_3$ group with the loss of one positive charge precludes the uptake of the compound in the cell nuclei. Because this information is essential for future drug design, it is important to mention here that identical observations were made using two other cell lines, P388 murine leukemia and HT29 human colon carcinoma (data not shown). The different cellular distribution properties of DB75 vs DB607 are absolutely not a unique feature of the B16 melanoma cell line used throughout this study.

The situation is comparable in the imidazoline series. The cell distribution profiles obtained with furimidazoline (DB60) are indistinguishable from that seen with furamidine (DB75). The conversion of the amidine into a five-membered cyclic form is known to enhance DNA intercalation as opposed to minor groove binding[12] but has no perceptible effect on cell distribution because both compounds accumulate in the nuclei. But here again, the replacement of one of the two imidazoline

groups with a methoxy group leads to a loss of nuclear uptake, and this is in perfect agreement with the above observations. The result is not as clear with DB606 as it is with DB607 because an excessively long exposure time was required to observe the cells under the microscope with DB606 (compared the exposure times for DB606 and DB607 in Table 1), but nevertheless, it can be seen clearly that this monocationic imidazoline compound is poorly taken up into the nuclei. Very limited nuclear uptake was also observed with the monocations in the phenylfuranbenzimidazole series. DB771 showed almost no cell uptake, and its imidazoline counterpart DB772 was considerably less concentrated in the nuclei of the cells than the corresponding dication DB302. Interestingly, the amidine DB771 shows a higher tendency to enter the nucleus than the corresponding imidazolidine DB772 (both the profiles and exposure times are different). A similar observation can be made when comparing the methoxy compounds, amidine DB607 vs imidazolidine DB606. The difference might be accounted for by their different capacities to bind to DNA. Previous DNA binding studies have revealed that the imidazolidines have a tendency to intercalate into GC-rich DNA sequences as well as into a favorable AT-specific minor groove interaction mode. The amidine derivatives display a much weaker ten-
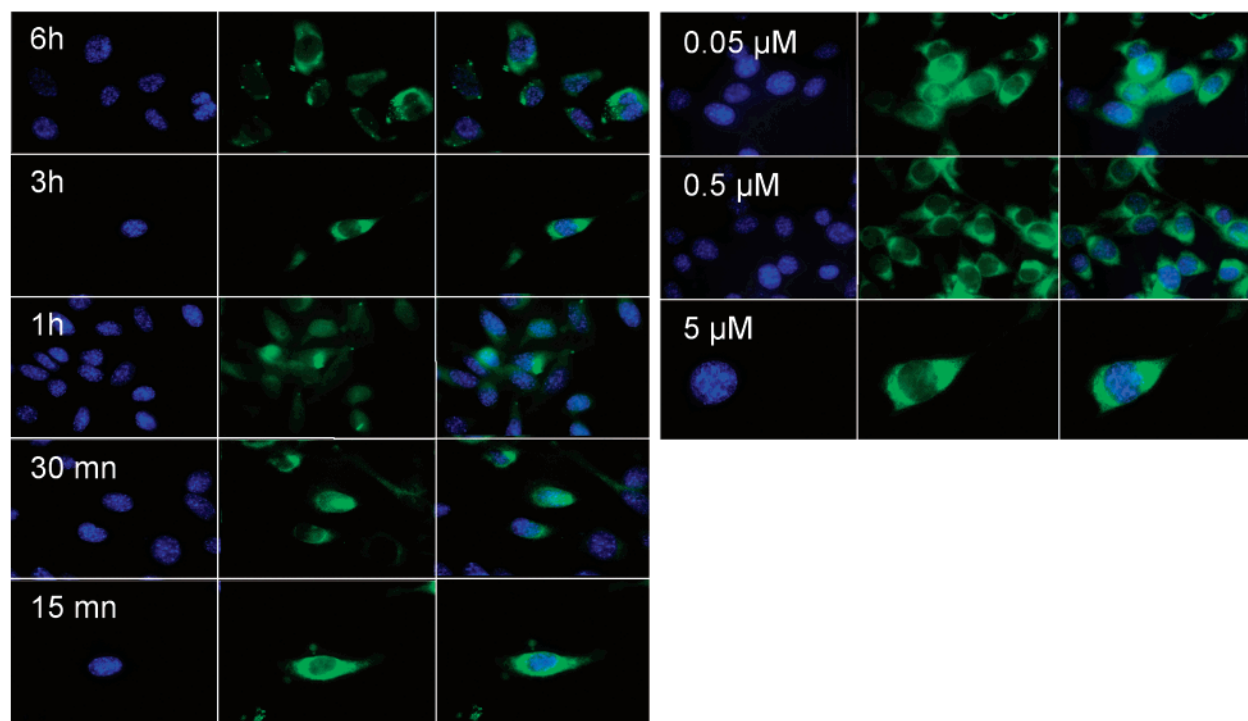
Figure 3. Fluorescence of B16 melanoma cells labeled with DB293. The cells were treated with 2 μM DB293 for 15 min to 6 h (left) or for 18 h with increasing concentrations of DB293 (right). Other details are as for Figure 2.

dency to intercalate and behave as much more specific minor groove binders in AT sequences.[12,17]

It is important to mention that upon binding to DNA, the fluorescence of these diamidines decreases (by about 20−25% for the groove binders, like DB75, and up to 70−90% for the compounds than can intercalate into DNA, like DB60). Therefore, the extent of nuclear uptake must be underestimated. The bright-blue fluorescence detected in the nuclei of the cells treated with compounds like DB75, DB60, and DB293 must reflect a massive nuclear accumulation.

The dications bearing either two amidines (DB75, DB293) or two imidazolidines (DB60, DB302) show highly preferential nuclear uptake, whereas the corresponding monocations accumulates preferentially into the cytoplasm of the cells (DB607) or they stain the cells very poorly, probably because they have difficulties entering the cells (DB771, DB772, DB606). The deletion of one of the two the amidine or imidazolidine groups or their substitution for methoxy groups reduces or abolishes nuclear uptake. Therefore, we may conclude that the presence of two positive charges favors nuclear uptake. However, there is an exception to the rule because the monocation DB501 with an amino group in place of the amidine of DB75 still shows preferential nuclear accumulation, but a long exposure time was required to detect this compound in the cells. The relatively weak intrinsic fluorescence of the monocations makes their detection in cells more difficult.

Interestingly, incubation of the cells with the extended compound DB182 produced a dense and bright accumulation of blue fluorescence in the nuclear region, demonstrating that the cells are capable of massive internalization of this tetracation. In the benzimidazole series, the tetracation DB340, which binds strongly and selectively to certain hairpin RNA,[18] also retains the ability to concentrate in the nuclei like DB75. In both

cases, the blue fluorescence was clearly concentrated in the nucleus of the cells with no apparent blue fluorescence in the cytoplasm. Therefore, the presence of four positive charges is clearly not an obstacle to the nuclear binding. The dimethylaminopropyl side chains of DB182 attached on the amidine moieties do not restrict the capacity of the drug to enter into the nuclei, but it seems that the transfer into the nucleus is entirely driven by the amidines. Indeed, the dication DB654, for which the amidine of DB182 has been replaced with an amide linkage, is practically not detected in the cells and no blue signal is detected in the nuclei of cells labeled with this compound. We conclude, therefore, that the amidine groups (or equivalent cyclic forms) are the key structural elements necessary for the accumulation of the drugs in the nuclear compartment.

DB293. The benzimidazole compound DB293 is clearly distinct from all other compounds of the present series in terms of DNA binding. We have recently shown that this compound forms a stacked dimer in the DNA minor groove[16] and preferentially recognizes ATGA sequences.[19,20] It represents a lead compound for the design of sequence-specific gene regulatory molecules.[21] For this reason, its cell uptake capacities were investigated in more detail. Figure 3 shows micrographs obtained from a kinetics experiment with this compound. A time course study was carried out with 1 μM DB293, but little or no differences was observed when the cells were incubated for 15 min or 6 h prior to fluorescence microscopy. The nuclear uptake is too fast to be monitored by this technique. In all cases, DB293 seems to have "privileged" access to the nucleus. In fact, nuclear staining with DB293 was observed in less than 5 min after the incubation began. Similarly, cell nuclei become fluorescent within minutes of exposure to DB75 (data not shown). The concentration dependence of the nuclear accumulation process was also studied. At a low

concentration (0.05 μM), the drug DB293 is exclusively detected in the cell nuclei with no distinct cytoplasmic staining. Raising the concentration 100-fold to 5 μM increased the fluorescence intensity but did not change the internalization profile. No blue fluorescence was observed in the cytoplasm, indicating that the drug is concentrated exclusively in the nuclei. This was further confirmed by means of confocal microscopy (data not shown).

Relation to Cytotoxicity and DNA Binding. A conventional tetrazolium-based MTS assay was applied to determine the drug concentration required to inhibit cell growth by 50% after incubation in the culture medium for 72 h. As indicated by the IC$_{50}$ values in Table 1, the cytotoxicity of the test compounds varies considerably from one to another and no direct relationship with the distribution profile can be proposed. For example, the tetracation DB340, which was found to enter efficiently into the nuclei of the B16 cells, is totally inactive whereas the other tetracation DB182 proved to be highly toxic to the cells under identical conditions. In general but not systematically, the compounds in the benzimidazole series are less toxic than those in the equivalent phenyl-containing analogues and the imidazoline compounds show higher toxicity compared to the amidines (e.g., DB60 vs DB75 and DB772 vs DB771). This general trend can be deduced from additional studies with a larger number of compounds (unpublished data).

The nuclei of B16 cells retain the dication DB75, where it would be expected to exert a cytotoxic effect. In contrast, the monocation does not enter the nuclei, but despite the lack of nuclear fluorescence in DB607-treated cells, the compound is among the most cytotoxic agents in the series. The IC$_{50}$ value measured with DB607 is even superior to that of DB75, indicating that no simple relationship exists among the level of nuclear-bound drug and intranuclear fluorescence intensity. Nuclear uptake is not associated with cytotoxicity.

To determine the relative affinities of the compounds used in the cell penetration studies for their DNA recognition sites, melting temperature (T_m) values of the compound–DNA complexes were compared to values for free DNA (Table 1). All of the compounds caused increases in the DNA T_m value, but the magnitude of the changes was quite different. The compounds fall into two different binding classes based on their T_m increases with DNA. The dications and tetracations all have T_m increases that are 24 °C or greater. This magnitude of T_m increase is consistent with binding constants in the range of 10^8 M^{-1} and higher for this set of compounds.[12,13,18] With the monocations, the T_m increases are much smaller and can be grouped between a 5 and 9 °C increase. This magnitude of increase is consistent with a binding constant below 10^5 M^{-1} for the compound–DNA complex. Clearly the dication and tetracation groups bind to the AT DNA recognition site approximately 1000 times more strongly than the monocations of corresponding structure. Interestingly, the only compound that clearly does not enter the nucleus, DB607, exhibits the weakest affinity for DNA, as judged from the melting temperature measurements performed with poly(dA)·(dT) (Table 1) and calf thymus DNA (data not shown). The other monocations also

interact with DNA much more weakly than the corresponding dimers. For example, the T_m values measured with DB293 are considerably higher than those obtained with DB771 containing one amidine group. But here again, we cannot deduce any direct relationship between DNA binding and cytotoxicity or cell distribution. As a consequence, it will be difficult to use direct imaging of diphenylfuran derivatives within cells to guide analogue screening for potentially advantageous antiproliferative properties. The degree of nuclear retention may be a secondary factor in determining cellular sensitivity to diphenylfurans. The nucleus may serve as a reservoir and perhaps as a slow-release device for furamidine-type compounds.

Discussion

The natural fluorescence of some drugs enables distribution of the molecules to be monitored both throughout the cell population and within intracellular compartments of intact viable cells. But the benefits of imaging fluorescent DNA-binding compounds in live cells have, until now, been underexploited. The cellular distribution of some fluorescent DNA intercalating drugs, in particular antitumor agents from the anthracycline and ellipticine families (e.g., daunomycin, adriamycin,[22,23] mitoxantrone,[24] ditercalinium[25]), has been investigated. But relatively few studies have been performed with nonintercalating drugs[26] and in particular with DNA minor groove binders. The dyes DAPI and Hoechst 33258/33342 have been shown to enter cell nuclei,[27–29] but as far as we know, there are no reports in the literature of structure cell distribution relationship studies. The present study is unique in comparing the cellular localization of a homogeneous series of DNA minor groove binders. These are the first data to show that this type of cationic ligand readily penetrates into cells and exhibits selective nuclear uptake capacity. The high degree of accumulation of DB75 into the cell nuclei is an essential component in the development of gene-targeted drugs.

The molecular mechanism(s) directing DB75 and DB293 to the nucleus remains unknown at present and awaits further investigation. These charged compounds enter cells rapidly, and a pure diffusion process seems unlikely. Specific transporters, analogous to those identified for the entry of the related drug pentamidine in parasites,[30] likely promote intracellular accumulation of these compounds. Normal and malignant cells possess a high-affinity transport system that controls the entry of polyamines (putrescine, spermidine, spermine) and guanidines (e.g., methylglyoxal bis(guanylhydrazone)).[31] This membrane transport system may well be exploited by the amidines to cross the plasma membrane. Interestingly, the potent accumulation of the DNA-binding dicationic compounds, like DB75 and DB293, in nuclei contrasts with the limited intracellular capacity of related polyamide-type minor groove binders. In a recent study with a fluorescently tagged DNA-binding polyamide related to distamycin, it was shown that the conjugate molecule selectively accumulates in mitochondria of adenocarcinoma SKOV-3 cells rather than in the nucleus.[32] No evidence of nuclear uptake was reported, and the selective mitochondrial uptake was attributed to the relatively high electronegativity of the mitochon-

drial membranes, which can restrict uptake of cationic compounds.[33] The findings reported here do not support this view and in contrast reveal that cationic drugs can be delivered selectively to the cell nucleus. The T_m studies in Table 1 suggest a correlation between DNA binding affinity and nuclear uptake for the furan-based compounds in this report. Apparently there is no direct relationship between nuclear accumulation and cytotoxicity in the cells tested in this study. Rather, the biological activity may depend on the capacity of these compounds to recognize specific sequences in DNA and consequently to affect the profiles of gene expression. The specific distribution of the diamidines within some critical portions of the genome is currently investigated. All results together indicate that amidine or related functions and strong DNA binding are required for significant nuclear uptake in this series.

Experimental Section

Synthesis. Compounds DB60 and DB75,[1] DB182,[34] DB293 and DB302,[35] DB340,[18] and DB501[19] have been previously described. The experimental protocols for the synthesis of compounds DB606, DB607, DB654, DB771, and DB772 are described below.

2,5-Bis[4-(4-chlorobutyramido)phenyl]furan. To a chilled solution of 2,5-bis(4-aminophenyl)furan[36] (0.50 g, 2.0 mmol) in dry acetonitrile (20 mL) was added triethylamine (0.42 g, 4.15 mmol) followed dropwise by 4-chlorobutyryl chloride (0.58 g, 4.1 mmol), and the resulting suspension was stirred at room temperature for 2 h. Water (20 mL) was then added, and the solid was collected, rinsed with water followed by methanol, and finally air-dried to give a light-tan solid (0.88 g, 96%), mp 268–269 °C. ^{1}H NMR (DMSO-d_6): δ 10.09 (broad s, 2H), 7.64–7.74 (partially coalescing dd, J = 9.0, 9.0 Hz, 8H), 6.92 (s, 2H), 3.70 (t, 4H), 2.40–2.50 (t, 4H, partially obscured by DMSO solvent), 2.00–2.14 (m, 4H). MS (EI), m/z: 386 (M − 2HCl).

2,5-Bis[4-[4-(dimethylamino)butyramido]phenyl]-furan Dihydrochloride (DB654). To a solution of the 4-chlorobutyramide (0.66 g, 1.44 mmol) and NaI (50 mg) in DMF (15 mL) was added 40% aqueous dimethylamine (7 mL). After the sealed mixture was stirred at room temperature for 1 week, excess brine solution was added and the precipitate was collected and dissolved in 1 N HCl. After extraction with EtOAc, the acidic aqueous layer was made basic (NaOH) and extracted again with EtOAc. This second extract was washed with brine, dried (MgSO₄), and concentrated to a solid that consisted of two spots on TLC. Column chromatrography (silica) eluting with EtOAc/MeOH/triethylamine (5:4:1) and collection of the more polar/slower-moving product gave, upon concentration of homogeneous fractions and trituration with ether, a light-tan solid (0.14 g, 20%), mp 218–220 °C. To prepare the dihydrochloride, a solution of the free base in EtOH (40 mL) was treated with anhydrous HCl and then was concentrated to near dryness to give a suspension. Following dilution with ether, the tan solid was collected and dried in vacuo. Yield: 0.16 g (20% overall). ^{1}H NMR (DMSO-d_6): δ 10.38 (broad s, 2H), 10.27 (s, 2H), 7.67–7.74 (coalescing dd, J = 9.0, 9.0 Hz, 8H), 6.92 (s, 2H), 2.75 (s, 6H), 3.05–3.10 (t, 4H), 2.43–2.49 (t, 4H, partially obscured by DMSO solvent), 1.94–2.02 (m, 4H). ^{13}C NMR (DMSO-d_6): δ 170.1, 152.2, 138.5, 125.2, 123.9, 119.4, 107.1, 56.0, 42.0, 33.0,19.7. MS (EI), m/z: 476 (M − 2HCl). Anal. Calcd for $C_{28}H_{36}N_4O_3 \cdot 2HCl$: C, H, N.

2-(2-Benzimidazolyl)-5-[4-cyanophenyl]furan. A mixture of 5-[4-cyanophenyl]-2-furancarboxaldehyde (1.97, 0.01 mol), 1,2-phenylenediamine (1.06 g, 0.01mol), and 1,4-benzoquinone (1.08 g, 0.01mol) in 50 mL of dry ethanol was heated at reflux (under nitrogen) for 8 h. The reaction mixture was cooled, diluted with ether, and filtered. The solid was collected and stirred with a 1:3 mixture of EtOH and ether for 20 min, and the yellow-brown solid was filtered, washed with ether, and dried in a vacuum at 70 °C for 12 h, which yielded 1.96 g

(69%), mp 227–228 °C dec. ^{1}H NMR (DMSO-d_6): δ 8.06 (d,-2H, J = 8.8 Hz), 7.91(d,2H, J = 8.8 Hz), 7.60 (dd,2H, J = 3.2, 6.4 Hz),7.38 (d, 1H, J = 3.6 Hz), 7.32(d, 1H, J = 3.6 Hz), 7.23 (dd,2H, J = 3.2, 6.4 Hz). ^{13}C NMR (DMSO-d_6): δ 152.1, 146.0, 142.7, 138.7, 133.2, 132.6, 124.1, 122.3, 118.4, 114.9, 112.5, 111.1, 109.8. MS, m/e: 285 (M⁺). Anal. Calcd for $C_{18}H_{11}N_3O$: C, H, N.

2-(2-Benzimidazolyl)-5-[4-(amidino)phenyl]furan Dihydrochloride (DB771). The above cyano compound (2.85 g, 0.01 mol) in 60 mL of ethanol was saturated with dry HCl gas at 0–5 °C. The reaction mixture was stirred at room temperature for 12 days (monitored by IR and TLC). The mixture was diluted with ether, and the yellow imidate ester hydrochloride was filtered, washed with ether, and dried under vacuum for 6 h, giving 3.73 g (92%) of solid. The solid was used in next step without further purification. A suspension of the imidate ester hydrochloride (0.808 g, 0.002 mol) in 35 mL of ethanol was saturated with ammonia gas at 0–5 °C and was stirred for 24 h at room temperature. The solvent was reduced to one-third under reduced pressure, diluted with ether, and filtered. The yellow solid was resuspended in 10 mL of ethanol, treated with 4 mL of saturated ethanolic HCl, and stirred at 35 °C for 2 h. The solvent was removed under vacuum, and the residue was triturated with ether, filtered, washed with ether, and dried under vacuum at 45 °C for 24 h to yield 0.61 g (81%) of a yellow solid, mp >280 °C dec. ^{1}H NMR (DMSO-d_6/D2): δ 8.15 (d, 2H, J = 8.7 Hz), 7.93 (d, 2H, J = 8.7 Hz), 7.78 (d, 1H, J = 3.6 Hz), 7.75 (dd, 2H, J = 3, 6.3 Hz), 7.50 (d, 1H, J = 3.6 Hz), 7.49 (dd, 1H, J = 3, 6.3 Hz). ^{13}C NMR (DMSO-d_6): δ 165.0, 155.9, 139.8, 139.7, 133.4, 132.4, 129.3, 127.8, 126.3, 125.2, 119.5, 114.3, 112.0. FAB-MS, m/e: 303 (M⁺ + 1). Anal. Calcd for $C_{18}H_{14}N_4O \cdot 2HCl$: C, H, N.

2-(2-Benzimidazolyl)-5-[4-(2-imidazolino)phenyl]furan Dihydrochloride (DB772). A mixture of the imidate ester hydrochloride (0.808 g, 0.002 mol) from above and ethylenediamine (0.12 g, 0.002 mol) in 20 mL of dry ethanol was heated at reflux for 12 h. The solvent volume was reduced to 8 mL under reduced pressure and diluted with ether. The resultant solid was filtered and dried. This solid was dissolved in 35 mL of hot ethanol and was saturated with HCl gas at room temperature. The mixture was stirred at 50 °C for 2 h and was concentrated under reduced pressure, and 30 mL of dry ether was added. The precipitated yellow salt was filtered, washed with ether, and dried under vacuum at 70 °C for 24 h to yield 0.69 g (84%) of a yellow solid, mp >300 °C dec. ^{1}H NMR (DMSO-d_6/D2): δ 8.06 (d, 2H, J = 8.7 Hz), 7.91 (d, 2H, J = 8.7 Hz), 7.71 (dd, 2H, J = 3, 6 Hz), 7.64 (d, 1H, J = 3.9 Hz), 7.47 (dd, 1H, J = 3, 6.3 Hz), 7.44 (d, 1H, J = 3.9 Hz), 3.94 (s, 4H). ^{13}C NMR (DMSO-d_6): δ 164.6, 155.7, 140.3, 140.1, 133.9, 132.9, 129.7, 126.7, 125.4, 122.1, 119.2, 114.6, 112.5, 44.8. FAB-MS, m/e: 303 (M⁺ + 1). Anal. Calcd for $C_{20}H_{16}N_4O \cdot 2HCl \cdot 0.5H_2O$: C, H, N.

1-(4-Bromophenyl)-4-(4-methoxyphenyl)butane-1,4-dione. To a stirred mixture of 1-(4′-bromophenyl)-3-dimethylaminopropane-1-one hydrochloride (14.0 g, 0.05 mol), 3-benzyl-5-(2-hydroxyethyl)-4-methylthiazolium chloride (0.68 g, 0.0025 mol), and triethylamine (15.15 g, 0.15 mol) in 200 mL of anhydrous dioxane was added 4-methoxybenzaldehyde (6.8 g, 0.05 mol), and the mixture was heated at reflux for 12 h (under nitrogen). The solvent was removed, and the residue was stirred with 200 mL of water. The gummy mass was extracted with 3 × 120 mL of warm chloroform, washed with 2 × 100 mL of 10% NaHCO₃, dried over Na₂SO₄, and filtered. Solvent was removed, and the residual mass was stirred with 30 mL of ether/ethanol (1:2) to yield a white crystalline solid, 6.1 g (35.3%), mp 121–123 °C. ^{1}H NMR (DMSO-d_6): δ 8.0 (d, 2H, J = 8.8 Hz), 7.88 (d, 2H, J = 8.8 Hz), 7.60 (d, 2H, J = 8.8 Hz), 6.94 (d, 2H, J = 8.8 Hz), 3.86 (s, 1H), 3.40–3.38 (m, 4H). ^{13}C NMR (DMSO-d_6): δ 197.8, 196.9, 136.2, 131.9, 130.4, 130.1, 129.7, 128.1, 113.8, 55.5, 32.6, 32.3. MS, m/e: 347 (M⁺). Anal. Calcd for $C_{17}H_{15}BrO_3$: C, H, N.

2-(4-Bromophenyl)-5-(4-methoxyphenyl)furan. A solution of the above diketone (5.55 g, 0.016 mol) in 150 mL of CHCl₃/CH₃OH (7:3) was saturated with dry HCl gas at 0–5

°C and was stirred at 25 °C for 2 h (monitored by TLC silica gel ether/CHCl$_3$, 7:3), and the solvent was removed under reduced pressure. The residue was stirred with water, and the solid was filtered, washed with water, resuspended in 10% NaHCO$_3$ (150 mL), filtered, washed with water, dried, and recrystallized from CHCl$_3$/ether (3:7) to give a white solid, 4.7 g (89%), mp 193−194 °C. ^{1}H NMR (DMSO-d_6): δ 7.65 (d, 2H, J = 8.8 Hz), 7.59 (d, 2H, J = 8.8 Hz), 7.51 (d, 2H, J = 8.8 Hz), 6.94 (d, 2H, J = 8.8 Hz), 6.77 (d, 1H, J = 3.6 Hz), 6.63 (d, 1H, J = 3.6 Hz), 3.84 (s, 3H). ^{13}C NMR (DMSO-d_6): δ 158.4, 152.8, 150.4, 130.8, 128.8, 124.2, 124.0, 122.5, 119.5, 113.4, 107.1, 104.9, 54.3. MS, m/e: 329 (M$^+$). Anal. Calcd for C$_{17}$H$_{13}$BrO$_2$: C, H, N.

2-(4-Cyanophenyl)-5-(4-methoxyphenyl)furan. A mixture of the above bromo analogue (4.6 g, 0.014 mol) and CuCN (1.87 g, 0.021 mol) in 60 mL of *N*-methyl-2-pyrrolidinone was heated at reflux (under nitrogen) for 2.5 h. The mixture was cooled, diluted with 100 mL water, and stirred with 100 mL of 10% NaCN(aq) for 3 h. The solid was filtered, washed with water, and dried, and the crude product was dissolved in chloroform and chromatographed over neutral alumina to yield a pale solid, 2.95 g (77%), mp 148−149 °C. ^{1}H NMR (DMSO-d_6): δ 7.93 (d,2H, J = 8.8 Hz), 7.83 (d, 2H, J = 8.8 Hz), 7.77 (d, 2H, J = 8.8 Hz), 7.25 (d, 1H, J = 3.6 Hz), 7.02 (d, 2H, J = 8.8 Hz), 6.95 (d,1H, J = 3.6 Hz), 3.81 (s, 3H). ^{13}C NMR (DMSO-d_6): δ 159.2, 154.3, 150.0, 133.9, 132.5, 125.2, 123.4, 122.4, 118.6, 111.4, 108.7, 106.6, 55.1. MS, m/e: 275 (M$^+$). Anal. Calcd for C$_{18}$H$_{13}$BrO$_2$: C, H, N.

2-(4-Amidinophenyl)-5-(4-methoxyphenyl)furan Hydrochloride (DB607). The above cyano compound (2.75 g, 0.01 mol) in 60 mL of ethanol was saturated with dry HCl gas at 0−5 °C. The reaction mixture was stirred at room temperature for 8 days (monitored by IR and TLC) and was diluted with ether. The yellow imidate ester hydrochloride was filtered, washed with ether, and dried under vacuum for 6 h to give 3.25 g (91%) of a solid. The solid was used in the next step without further purification. A suspension of the imidate ester hydrochloride (1.07 g, 0.003 mol), in 25 mL of ethanol was saturated with ammonia gas at 0−5 °C and was stirred for 24 h at room temperature. The solvent was removed under reduced pressure, diluted with water, and basified with 2 N NaOH(aq) to pH 10. The solid was filtered, washed with water, and dried. The solid was dissolved in 15 mL of ethanol, treated with 2 mL of saturated ethanolic HCl, and stirred at 35 °C for 2 h. The solvent was removed under reduced pressure, and the residue was triturated with ether, filtered, washed with ether, and dried under vacuum at 45 °C for 24 h to yield 0.66 g (67%) of a yellow solid, mp >280 °C dec. ^{1}H NMR(DMSO-d_6): δ 9.44 (br, 2H), 9.29 (br, 2H), 9.26 (br, 2H), 7.98 (d, 2H, J = 8.8 Hz), 7.95 (d, 2H, J = 8.8 Hz), 7.78 (d, 2H, J = 8.8 Hz), 7.29 (d, 2H, J = 8.8 Hz), 7.02 (d, 2H, J = 8.8 Hz), 6.97 (d, 1H, J = 3.6 Hz), 3.80 (s, 3H). ^{13}C NMR (DMSO-d_6): δ 164.9, 159.2, 154.2, 150.2, 134.7, 128.6, 125.4, 125.3, 122.4, 114.4, 111.2, 106.7, 55.1. FAB-MS, m/e: 293 (M$^+$ + 1). Anal. Calcd for C$_{18}$H$_{16}$N$_2$O$_2$·1HCl: C, H, N.

2-[4-(2-Imidazolyl)phenyl]-4-(methoxyphenyl)furan Hydrochloride (DB606). A mixture of the imidate ester hydrochloride (1.07 g, 0.003 mol) from above and ethylenediamine (0.18 g, 0.003 mol) in 30 mL of dry ethanol was heated at reflux for 12 h. The solvent was distilled under reduced pressure. The solid was suspended in 50 mL of water, and the pH was adjusted to 10 with 2 N NaOH(aq). The solid was filtered, washed with water, and dried to yield the crystalline free base (72%), mp 159−160 °C. The solid was dissolved in 15 mL of hot ethanol and was saturated with HCl gas at 0 °C. The mixture was stirred at 50 °C for 2 h, and 30 mL of dry ether was added. The precipitated salt was filtered, washed with ether, and dried under vacuum at 70 °C for 24 h to yield 0.78 g (73%) of a yellow crystalline solid, mp >300 °C dec. ^{1}H NMR (DMSO-d_6): δ 10.8 (br, 2H), 8.16 (d, 2H, J = 8.8 Hz), 7.99 (d, 2H, J = 8.8 Hz), 7.78 (d, 2H, J = 8.8 Hz), 7.31 (d, 1H, J = 3.6 Hz), 7.02 (d, 2H, J = 8.8 Hz), 6.97 (d, 1H, J = 3.6 Hz), 3.99 (s, 3H), 3.81 (s, 3H). ^{13}C NMR (DMSO-d_6): δ 164.0, 159.2, 154.5, 150.0, 135.1, 129.2, 125.3, 123.0, 122.3, 119.7, 114.3, 111.7,

106.7, 55.1, 44.0. FAB-MS, m/e: 319 (M$^+$ + 1). Anal. Calcd for C$_{20}$H$_{18}$N$_2$O$_2$·1HCl: C, H, N.

Cell Cultures and Survival Assay. B16 melanoma cells were obtained from Dr. M.-C. De Pauw (University of Liège, Belgium). The melanocytes were maintained as monolayers in 150 cm^2 culture flasks using culture medium consisting of DMEM-glutaMAX medium supplemented with 10% fetal bovine serum, penicillin (100 IU/mL), and streptomycin (100 µg/mL). Cells were grown in a humidified atmosphere at 37 °C under 5% CO$_2$. In the exponential phase, the doubling time of these melanocytes ranged from 15 to 18 h and the confluence stage was achieved at a cell density of 3×10^5 cells/cm^2. B16 cells were harvested by trypsinization and plated 20 h before treatment with the test drug. The cytotoxicity of the drugs was assessed using a cell proliferation assay developed by Promega (CellTiter 96 AQ$_{ueous}$ one solution cell proliferation assay). Briefly, 2×10^4 exponentially growing cells were seeded in 96-well microculture plates with various drug concentrations in a volume of 100 µL. After 72 h of incubation at 37 °C, a total of 20 µL of MTS[37] was added to each well and the samples were incubated for a further 3 h at 37 °C. Plates were analyzed on a Labsystems Multiskan MS reader at 492 nm.

Fluorescence Microscopy. The cells (20 000 cells/cm^2) were incubated at 37 °C with the test compound, usually at 2 µM for 18 h unless otherwise stated. The medium was removed, and cells were rinsed with ice-cold PBS (10 min) prior to fixation with a 2% paraformaldehyde solution for 20 min at 4 °C. After being washed, the cells were incubated with fluorescent probes DiOC$_6$ (20 nM, 3,3-dihexyloxacarbocyanine iodide, Molecular Probes, Inc.) for 5 min at 37 °C in the dark, washed again with PBS, and then incubated with a solution of propidium iodide (0.2 µg/mL) for 5 min at room temperature. A drop of antifade solution was added, and the treated portion of the slide was covered with a glass coverslip. The fluorescence of the drug was detected and localized by fluorescence microscopy using a Zeiss microscope with a ×63 or ×100 oil objective. Images were captured using the software Quips Smart Capture (Vysis).

DNA Thermal Melting. Thermal melting experiments were conducted with Cary 3 and Cary 4 spectrophotometers interfaced to microcomputers as previously described.[38] MES10 buffer [10 mM 2-(*N*-morpholino)ethanesulfonic acid, 1 mM EDTA, pH 6.25 with 0.1 M NaCl] was used in the experiments with poly(dA)·(dT). A thermistor fixed to a reference cuvette was used to monitor the temperature. In T_m experiments, DNA was added to buffer in 1 cm path length reduced volume quartz cells, and the concentration was determined by measuring the absorbance at 260 nm. The experiments were generally conducted at a concentration of 5×10^{-5} M DNA base pairs and a ratio of 0.6 compound per base pair of DNA.

References

(1) Das, B. P.; Boykin, D. W. Synthesis and antiprotozoal activity of 2,5-bis(4-guanylphenyl)furans. *J. Med. Chem.* **1977**, *20*, 531−536.

(2) Steck, E. A.; Kinnamon, K. K.; Davidson, D. E.; Duxbury, R. E.; Johnson, A. J.; Masters, R. E. *Trypanosoma rhodesience.* Evaluation of the antitrypanosomal action of 2,5-bis(4-guanylphenyl)furan dihydrochloride. *Exp. Parasitol.* **1982**, *53*, 133−144.

(3) Boykin, D. W.; Kumar, A.; Bender, B. K.; Hall, J. E.; Tidwell, R. R. Anti-*pneumocystis* activity of bis-amidoximes and bis-*O*-alkylamidoximes prodrugs. *Bioorg. Med. Chem. Lett.* **1996**, *6*, 3017−3021.

(4) Neidle, S.; Kelland, L. R.; Trent, J. O.; Simpson, I. J.; Boykin, D. W.; Kumar, A.; Wilson, W. D. Cytotoxicity of bis(phenylamidinium)furan alkyl derivatives in human tumour cell lines: Relation to DNA minor groove binding. *Bioorg. Med. Chem.* **1997**, *7*, 1403−1408.

(5) Dykstra, C. C.; McClernon, D. R.; Elwell, L. P.; Tidwell, R. R. Selective inhibition of topoisomerases from *Pneumocystis carinii* versus topoisomerases from mammalian cells. *Antimicrob. Agents Chemother.* **1994**, *38*, 1890−1898.

(6) Hildebrant, E.; Boykin, D. W.; Kumar, A.; Tidwell, R. R.; Dystra, C. C. Identification and characterization of an endo/exonuclease in *Pneumocystis carinii* that is inhibited by dicationic diarylfurans with efficacy against *Pneumocystis pneumonia*. *J. Eukaryotic Microbiol.* **1998**, *45*, 112−121.

(7) Bailly, C.; Dassonneville, L.; Carrasco, C.; Lucas, D.; Kumar, A.; Boykin, D. W.; Wilson, W. D. Relationships between topoisomerase II inhibition, sequence-specificity and DNA binding mode of dicationic diphenylfuran derivatives. *Anti-Cancer Drug Des.* **1999**, *14*, 47−60.

(8) Salvioli, S.; Ardizzoni, A.; Franceschi, C.; Cossarizza, A. JC-1, but not DiOC$_6$(3) or rhodamine 123, is a reliable fluorescent probe to assess $\Delta\Psi$ changes in intact cells: implications for studies on mitochondrial functionality during apoptosis. *FEBS Lett.* **1997**, *411*, 77−82.

(9) Kluza, J.; Lansiaux, A.; Wattez, N.; Mahieu, C.; Osheroff, N.; Bailly, C. Apoptotic response of HL-60 human leukemia cells to the antitumor drug TAS-103. *Cancer Res.* **2000**, *60*, 4077−4084.

(10) Facompré, M.; Wattez, N.; Kluza, J.; Lansiaux, A.; Bailly, C. Relationship between cell cycle changes and variations of the mitochondrial membrane potential induced by etoposide. *Mol. Cell Biol. Res. Commun.* **2000**, *4*, 37−42.

(11) Trent, J. O.; Clark, G. R.; Kumar, A.; Wilson, W. D.; Boykin, D. W.; Hall, J. E.; Tidwell, R. R.; Blagburn, B. L.; Neidle, S. Targeting the minor groove of DNA: crystal structures of two complexes between furan derivatives of berenil and the DNA dodecamer d(CGCGAATTCGCG)$_2$. *J. Med. Chem.* **1996**, *39*, 4554−4562.

(12) Wilson, W. D.; Tanious, F. A.; Ding, D.; Kumar, A.; Boykin, D. W.; Colson, P.; Houssier, C.; Bailly, C. Nucleic acid interactions of unfused aromatic cations: Evaluation of proposed minorgroove, major-groove, and intercalation binding modes. *J. Am. Chem. Soc.* **1998**, *120*, 10310−10321.

(13) Mazur, S.; Tanious, F. A.; Ding, D.; Kumar, A.; Boykin, D. W.; Simpson, I. J.; Neidle, S.; Wilson, W. D. A thermodynamic and structural analysis of DNA minor groove complex formation. *J. Mol. Biol.* **2000**, *300*, 321−337.

(14) Oszczapowicz, J. In *The Chemistry of Amidines and Imidates*; Patai, S., Rappoport, Z., Ed.; John Wiley & Sons, Ltd.: Chichester, U.K., 1991; Vol. 2, pp 623−688.

(15) Haeflinger, G.; Kuske, F. K. H. In *The Chemistry of Amidines and Imidates*; Patai, S., Rappoport, Z., Ed.; John Wiley & Sons, Ltd.: Chichester, U.K., 1991; Vol. 2, pp 1−100.

(16) Wang, L.; Bailly, C.; Kumar, A.; Ding, D.; Bajic, M.; Boykin, D. W.; Wilson, W. D. Specific molecular recognition of mixed nucleic acid sequences: An aromatic dication that binds in the DNA minor groove as a dimer. *Proc. Natl. Acad. Sci. U.S.A.* **2000**, *97*, 12−16.

(17) Nguyen, B.; Tardy, C.; Bailly, C.; Colson, P.; Houssier, C.; Kumar, A.; Boykin, D. W.; Wilson, W. D. Influence of compound structure on affinity, sequence selectivity and mode of binding to DNA for unfused aromatic dications related to furamidine. *Biopolymers*, in press.

(18) Li, K.; Davis, T. M.; Bailly, C.; Kumar, A.; Boykin, D. W.; Wilson, W. D. A heterocyclic inhibitor of the Rev−RRE complex binds to RRE as a dimer. *Biochemistry* **2001**, *40*, 1150−1158.

(19) Wang, L.; Carrasco, C.; Kumar, A.; Stephens, C. E.; Bailly, C.; Boykin, D. W.; Wilson, W. D. Evaluation of the influence of compound structure on stacked-dimer formation in the DNA minor groove. *Biochemistry* **2001**, *40*, 2511−2521.

(20) Bailly, C.; Tardy, C.; Wang, L.; Armitage, B.; Hopkins, K.; Kumar, A.; Schuster, G. B.; Boykin, D. W.; Wilson, W. D. Recognition of ATGA sequences by the unfused aromatic dication DB293 forming stacked dimers in the DNA minor groove. *Biochemistry* **2001**, *40*, 9770−9779.

(21) Wilson, W. D.; Wang, L.; Tanious, F.; Kumar, A.; Boykin, D. W.; Carrasco, C.; Bailly, C. BIAcore and DNA footprinting for discovery and development of new DNA targeted therapeutics and reagents. *Biacore J.* **2001**, *1*, 15−19.

(22) Egorin, M. J.; Hildebrand, R. C.; Cimino, E. F.; Bachur, N. R. Cytofluorescence localization of adriamycin and daunomycin. *Cancer Res.* **1974**, *34*, 2243−2245.

(23) Marquardt, D.; Center, M. S. Drug transport mechanism in HL60 cells isolated for resistance to adriamycin: Evidence for nuclear drug accumulation and redistribution in resistant cells. *Cancer Res.* **1992**, *52*, 3157−3163.

(24) Smith, P. J.; Sykes, H. R.; Fox, M. E.; Furlong, I. J. Subcellular distribution of the anticancer drug mitoxantrone in human and drug-resistant murine cells analyzed by flow cytometry and confocal microscopy and its relationship to the induction of DNA damage. *Cancer Res.* **1992**, *52*, 4000−4008.

(25) Fellous, R.; Coulaud, D.; El Abed, I.; Roques, B. P.; Le Pecq, J. B.; Delain, E.; Gouyette, A. Cytoplasmic accumulation of ditercalinium in rat hepatocytes and induction of mitochondrial damages. *Cancer Res.* **1988**, *48*, 6542−6549.

(26) Brangi, M.; Litman, T.; Ciotti, M.; Nishiyama, K.; Kohlhagen, G.; Takimoto, C.; Robey, R.; Pommier, Y.; Fojo, T.; Bates, S. E. Camptothecin resistance: role of the ATP-binding cassette (ABC), mitoxantrone-resistance half-transporter (MXR), and potential for glucuronidation in MXR-expressing cells. *Cancer Res.* **1999**, *59*, 5938−5946.

(27) Morgan, S. A.; Watson, J. V.; Twentyman, P. R.; Smith, P. J. Reduced nuclear binding of a DNA minor groove ligand (Hoechst 33342) and its impact on cytotoxity in drug resistant murine cell lines. *Br. J. Cancer* **1990**, *62*, 959−965.

(28) Lahmy, S.; Viallet, P.; Salmon, J. M. Is reduced accumulation of Hoechst 33342 in mutlidrug resistant cells related to P-glycoprotein activity? *Cytometry* **1995**, *19*, 126−133.

(29) Harapanhalli, R. S.; McLaughlin, L. W.; Howell, R. W.; Rao, D. V.; Adelstein, S. J.; Kassis, A. I. [^{125}I/^{127}I]iodoHoechst 33342: synthesis, DNA binding, and biodistribution. *J. Med. Chem.* **1996**, *39*, 4804−4809.

(30) De Koning, H. P. Uptake of pentamidine in *Trypanosoma brucei brucei* is mediated by three distinct transporters: Implications for cross-resistance with arsenicals. *Mol. Pharmacol.* **2001**, *59*, 586−592.

(31) Ekelund, S.; Nygren, P.; Larsson, R. Guanidino-containing drugs in cancer chemotherapy: biochemical and clinical pharmacology. *Biochem. Pharmacol.* **2001**, *61*, 1183−1193.

(32) Sharma, S. K.; Morrissey, A. T.; Miller, G. G.; Gmeiner, W. H.; Lown, J. W. Design, synthesis, and intracellular localization of a fluorescently labeled DNA binding polyamide related to the antibiotic distamycin. *Bioorg. Med. Chem. Lett.* **2001**, *11*, 769−772.

(33) Johnson, L. V.; Walsh, M. L.; Chen, L. B. Localization of mitochondria in living cells with rhodamine 123. *Proc. Natl. Acad. Sci. U.S.A.* **1980**, *77*, 990−994.

(34) Zhao, M.; Ratmeyer, L.; Peloquin, R. G.; Yao, S.; Kumar, A.; Spychala, J.; Boykin, D. W.; Wilson, W. D. Small changes in cationic substituents of diphenylfuran derivatives have major effects on the binding affinity and the binding mode with RNA helical duplexes. *Bioorg. Med. Chem.* **1995**, *3*, 785−794.

(35) Hopkins, K. T.; Wilson, W. D.; Bender, B. C.; McCurdy, D. R.; Hall, J. E.; Tidwell, R. R.; Kumar, A.; Bajic, M.; Boykin, D. W. Extended aromatic furan amidino derivatives as anti-*Pneumocystis carinii* agents. *J. Med. Chem.* **1998**, *41*, 3872−3878.

(36) Stephens, C. E.; Tanious, F.; Kim, S.; Wilson, W. D.; Schell, W. A.; Perfect, J. R.; Franzblau, S. G.; Boykin, D. W. Diguanidino and "reversed" diamidino 2,5-diarylfurans as antimicrobial agents. *J. Med. Chem.* **2001**, *44*, 1741−1748.

(37) Cory, A. H.; Owen, T. C.; Barltrop, J. A.; Cory, J. G. Use of an aqueous soluble tetrazolium/formazan assay for cell growth assays. *Cancer Commun.* **1991**, *3*, 207−212.

(38) Wilson, W. D.; Tanious, F. A.; Fernandez-Saiz, M.; Rigl, C. T. Evaluation of drug−nucleic acid interactions by thermal melting curves. *Methods Mol. Biol.* **1997**, *90*, 219−240.

JM010539N